J Mol Model (2008) 14:465–470
DOI 10.1007/s00894-008-0304-1

ORIGINAL PAPER

Geometric and electronic structures of new endohedral fullerenes: Eu@C_{72}

Mei Chi · Zhuxia Zhang · Peide Han · Xiaohong Fang · Wei Jia · Hongbiao Dong · Bingshe Xu

Received: 14 November 2007 / Accepted: 14 March 2008 / Published online: 15 April 2008

Abstract The geometric and electronic structures of rare earth metallofullerenes Eu@C_{72} were investigated using density functional theory (DFT) within a generalized gradient approximation (GGA). The geometric optimization revealed that the most favorable endohedral site for Eu is off-center along the C_2 axis on the σ_v plane pointing to the (5, 5) bond at the fusion of two pentagons. Calculations for electronic structures show that two 6s electrons in Eu transfer to the lowest-unoccupied-molecular orbitals of C_{72} while 4f electrons remain in Eu.

Keywords Metallofullerenes · Eu@C_{72} · Density functional theory

Introduction

Fullerenes are closed-shell molecular cages made up of carbon atoms that are connected together to form five- and six-membered rings [1–3]. Most fullerenes obey the so-called isolated pentagon rule (IPR), which means that each pentagon is surrounded by five hexagons. In general, this arrangement is the most stable because neighboring pentagons increase the strain in the system and disrupt the ideal carbon–carbon bonding pattern. The IPR has proved particularly valuable in unraveling the cage structures of higher fullerenes and metallofullerenes [4–9]. Fullerenes, if they violate this rule, are believed to be unstable and difficult to isolate. However, deviations from the IPR are have sometimes been found in some experimental studies of endohedral fullerenes such as Sc_2@C_{66} [10], Sc_3C@C_{68} [11, 12], Tb_3N@C_{84} [13], etc. Theoretical investigations of C_{72} [14], Ca@C_{72} [15] and Mg@C_{72} [16] also suggest that non-IPR cage structures are more stable than the IPR-satisfying structure. Recently, as the first proven structure of the C_{72} family, La@C_{72} was isolated and characterized by Wakahara et al. [17]. Experimental and DFT results suggested that La@C_{72} has a non-IPR C_2 cage and that the encapsulated La atom locates near the adjacent pentagons [17, 18]. These studies revealed that the inner metal atom(s) is(are) bonded to the fused pentagons, and electrons transfer from the inner metal core to the carbon cage, which change the electronic structures of the carbon cage, leading to the stabilization of the non-IPR fullerenes and conferring their special properties.

The rare earth element europium (Eu) has the electronic configuration $(Xe)^{54}(4f)^7(6s)^2$ and its classical chemistry involves the +2 and +3 redox states. A series of compounds activated by the Eu ion have been studied for their practical application as phosphorescent materials [19, 20]. The interaction between the Eu ion and carbon cages might influence the spectrum and lead to a new matrix of luminescence. Since the successful extraction of Eu@C_{74} in 1998 [21], europium endohedral metallofullerenes have attracted special attention because of their potentially

M. Chi · Z. Zhang · P. Han · X. Fang · W. Jia · B. Xu
Key Laboratory of Interface Science and Engineering in Advanced Materials, Taiyuan University of Technology, Ministry of Education,
Taiyuan, People's Republic of China

M. Chi · Z. Zhang · P. Han · W. Jia · B. Xu (✉)
College of Materials Science and Engineering,
Taiyuan University of Technology,
Taiyuan 030024, People's Republic of China
e-mail: xubs@public.ty.sx.cn

X. Fang
College of Mining Engineering,
Taiyuan University of Technology,
Taiyuan 030024, People's Republic of China

H. Dong
Department of Engineering, University of Leicester,
Leicester LE1 7RH, UK

luminescence properties, which cannot be expected from empty fullerenes [22, 23]. Very recently, endohedral fullerence Eu@C_{72} was successfully synthesized and separated by Bucher et al. [24, 25]. Two isomers were separated by HPLC and identified by LDI-TOF mass spectrometry; however, detailed information on their structural and electronic properties is still unknown. In this study, density functional theory (DFT) calculations were performed on Eu@C_{72} in order to better understand the experiments of Bucher et al. and to explore the structural and electronic properties of the cluster.

Methods

All DFT computations of C_{72} and Eu@C_{72} were performed using Dmol^3 code [26–28] with Perdew-Wang's 1991 generalized gradient approximation (GGA) function (PW91) [29]. An all-electron double-numerical basis set with polarization functions (DNP) was applied for all empty and endohedral cages. It is known that relativistic effects play an important role in the chemical and physical properties of molecules containing heavier elements such as europium. To take into account relativistic effects, we chose the all-electron scalar relativistic method for all calculations, utilizing the Douglas-Kroll-Hess (DKH) Hamiltonian [30], which is the most accurate approach available in the Dmol^3 package. A self-consistent field procedure was carried out, with a convergence criterion of 10^{-6} a.u. on energy and electron density, and geometry optimizations were performed under the symmetry constraint with a convergence criterion of 10^{-3} a.u. on gradient, 10^{-3} a.u. on displacement, and 10^{-5} a.u. on energy.

According to the research of Nagase et al. [31], three cages were considered in this paper, namely, one IPR cage with D_{6d} symmetry and two non-IPR isomers containing one fused pentagon with C_{2v} and C_2 symmetry, respectively. By placing the Eu atom at different sites among these isomers, nine configurations of Eu@C_{72} were obtained. For the IPR cage, two sites were given: (1) in the center (Eu@C_{72}−1); (2) off-center on the σ_d plane (Eu@C_{72}−2). For the C_{2v} cage, four different positions of the Eu atom were considered: (3) in the center (Eu@C_{72}−3); (4) off-center site along the C_2 axis on the σ_v plane pointing to the (5, 5) bond, the fusion of two pentagons (Eu@C_{72}−4); (5) off-center site along the C_2 axis on the σ_v plane pointing to the (6, 6) bond, the fusion of two hexagons (Eu@C_{72}−5); (6) off-center site along the axis vertical to the C_2 axis under a pentagon center on the σ_v plane (Eu@C_{72}−6). The positions of the Eu atom in the C_2 cage are: (7) in the center (Eu@C_{72}−7); (8) off-center site along the C_2 axis pointing to the (5, 5) bond, the fusion of two pentagons (Eu@C_{72}−8) and (9) off-center site along the C_2 axis pointing to the (6, 6) bond, the fusion of two hexagons (Eu@C_{72}−9). Figure 1 shows the nine possible structures of Eu@C_{72}.

Results and discussion

Relative stability of C_{72} isomers

Considering the neutral order first, C_{2v} C_{72} with one pentagon–pentagon fusion has the lowest energy, followed by the D_{6d} IPR isomer (65.39 kJ mol^{-1} higher in energy) and C_2 C_{72} (79.05 kJ mol^{-1} higher in energy) (Table 1). The isomeric stability is in quite good agreement with the

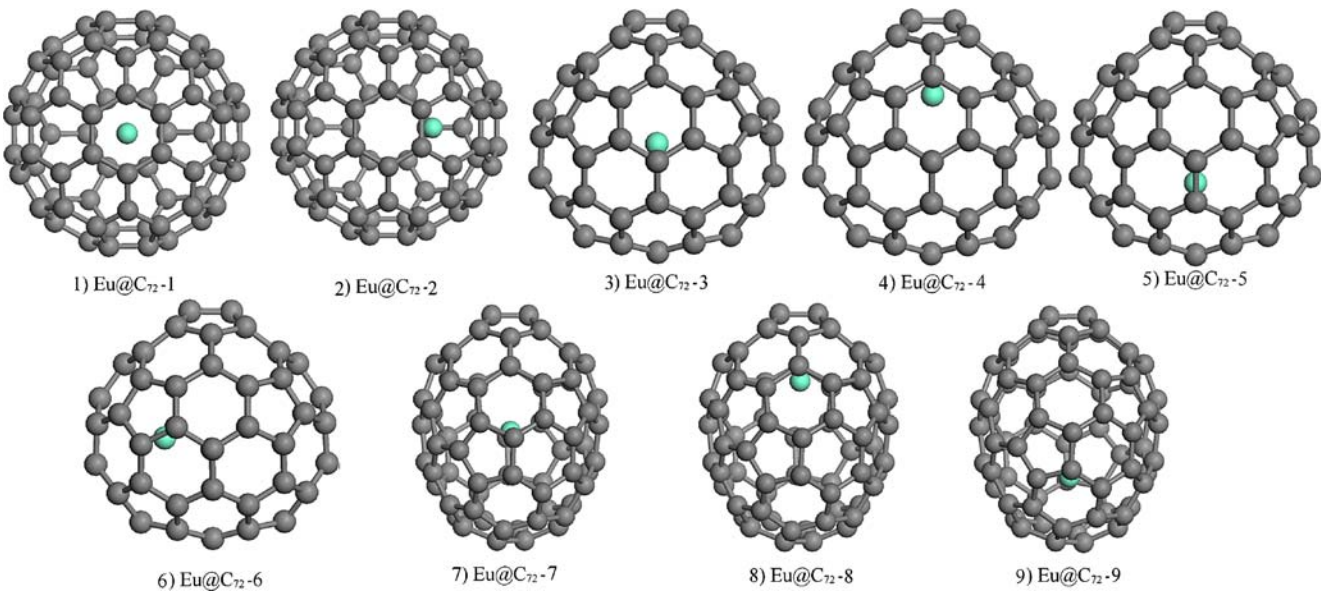

Fig. 1 Nine possible exohedral configurations for Eu@C_{72}. *Green ball* Europium (Eu), *gray balls* the cage

Table 1 Number of pentagon–pentagon fusions (N_{pp}), and the PW91/DNP relative energies of C_{72} and C_{72}^{2-}

Isomer	N_{pp}	C_{72} E_{rel} (kJ mol^{-1})	C_{72}^{2-} E_{rel} (kJ mol^{-1})
D_{6d}	0	65.39	109.25
C_{2v}	1	0	0
C_2	1	79.05	13.13

result in [14], in which Becke's three parameter function combined with the non-local Lee-Yang-Parr correlation function (B3LYP) in the standard 3–21G basis set was used. The screening of a metallofullerene structure usually begins by considering the charged empty cages; the magnitude of the negative charge is based on the expected electron donation from the encapsulated metal. Since the electronic structure of Eu@C_{72} can be described as Eu^{2+}@C_{72}^{2-} [24, 25], the C_{72}^{2-} isomers were also computed. While the stability order of C_{72} dianions changes, the stablest isomer is still the non-IPR isomer C_{2v}, followed by the C_2 (relative energy 13.13 kJ mol^{-1}). The IPR isomer becomes the most unstable, with a markedly higher relative energy (109. kJ mol^{-1}).

Relative stability of Eu@C_{72} isomers

Table 2 presents the HOMO, LUMO, E_{gap}, and binding energy (BE) of all nine isomers shown in Fig. 1. Commonly, the thermodynamic stability of the fullerene cage is determined by the BE, which is defined as the absolute value of the difference between the total energy of the molecule and the energy sum of all free atoms constituting the molecule. Obviously, Eu@C_{72}−4 has the lowest BE of −547.49 eV, followed by Eu@C_{72}−7. So, the most stable site for the Eu atom is the off-center site along the C_2 axis on the σ_v plane pointing to the (5, 5) bond, the fusion of two pentagons in the C_{2v} cage. One more thing worth noting is that the Eu atom in the center of the C_2 cage moves to the Eu site in Eu@C_{72}−7 during optimization. Eu@C_{72}−7 and Eu@C_{72}−8 converge to the same structure.

Table 2 The highest-occupied-molecular orbital (HOMO), lowest-unoccupied-molecular orbital (LUMO), E_{gap}, and binding energy (BE) of the nine Eu@C_{72} isomers (in eV)

Isomers	BE	HOMO	LUMO	E_{gap}
Eu@C_{72}−1	−544.10	−4.88	−4.72	0.16
Eu@C_{72}−2	−545.93	−4.98	−4.73	0.25
Eu@C_{72}−3	−545.23	−5.14	−5.02	0.12
Eu@C_{72}−4	−547.49	−5.18	−4.73	0.45
Eu@C_{72}−5	−546.28	−5.31	−4.87	0.44
Eu@C_{72}−6	−546.71	−5.14	−4.94	0.20
Eu@C_{72}−7	−547.31	−5.45	−4.81	0.64
Eu@C_{72}−8	−547.31	−5.45	−4.81	0.64
Eu@C_{72}−9	−546.29	−5.32	−5.00	0.32

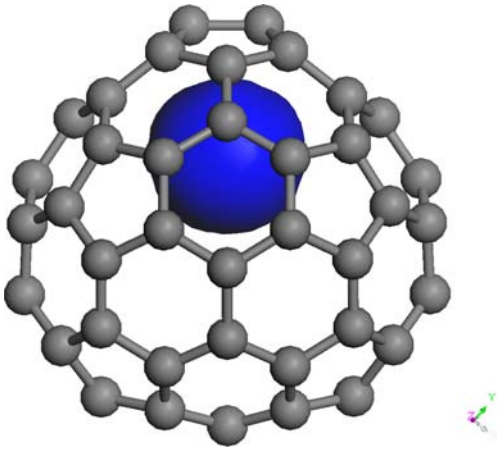

Fig. 2 Electron spin density of Eu@C_{72}−4, the illustrated hypersurface corresponding to a value of 0.01 e au^{-3}

We also compared the E_{gap} values of all the considered structures, because the E_{gap} value is often correlated with kinetic stability. The E_{gap} values calculated for the hollow cages are 1.45, 0.66 and 0.30 eV for D_{6d}, C_{2v} and C_2 C_{72}, respectively. It can be seen from Table 2 that, among the nine structures, Eu@C_{72}−7 has the largest E_{gap}, so it is expected to be the most stable kinetically. On the other hand, Eu@C_{72}−3 has the smallest E_{gap} of 0.12 eV and is therefore regarded as the most unstable kinetically. Moreover, except for the C_2 isomer, the E_{gap} values of the D_{6d} and C_{2v} cages are slightly reduced by encaging the Eu atom.

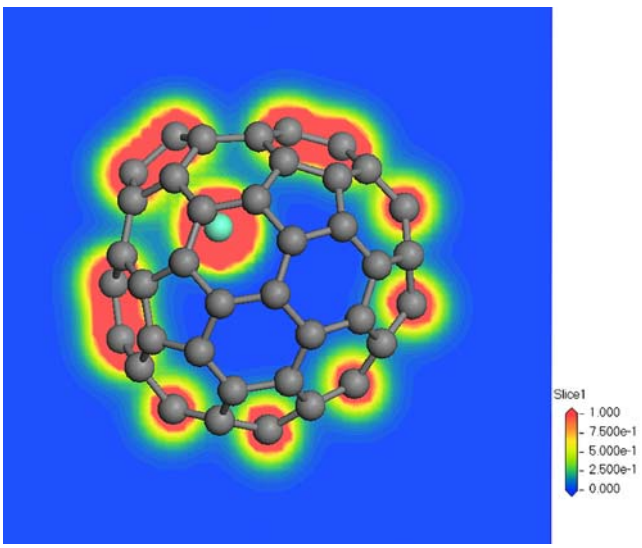

Fig. 3 Electronic density in the plane passing through the Eu ion in Eu@C_{72}−4

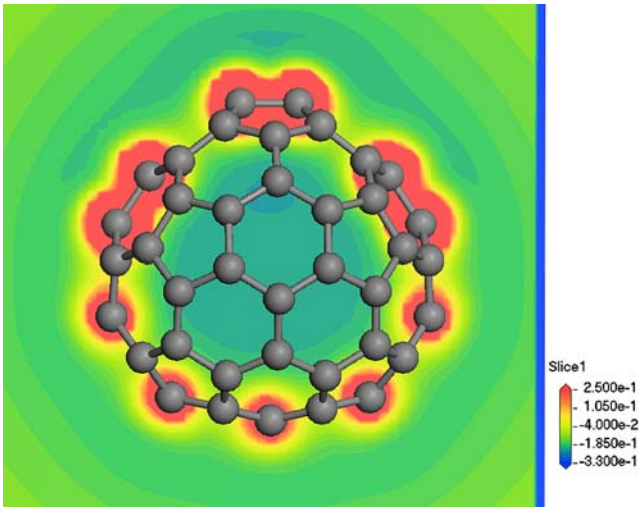

Fig. 4 Electrostatic potential map for C_{72}^{2-} in the plane passing through the σ_v plane

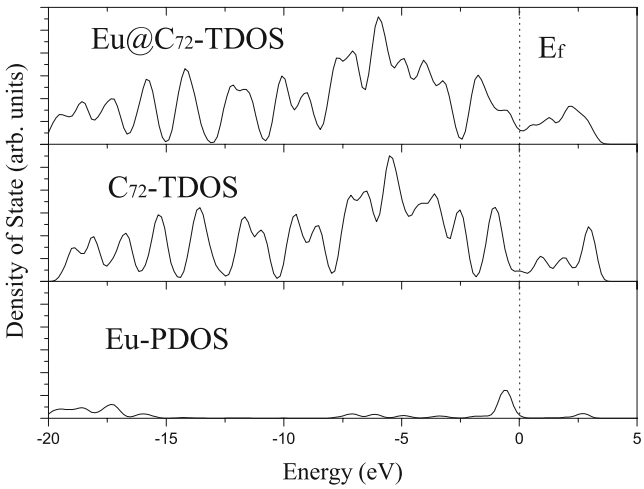

Fig. 6 The total density of state (TDOS) of C_{72}, Eu@C_{72}−4, and partial density of state (PDOS) of Eu in Eu@C_{72}−4. *Dotted line* Fermi energy in units of eV

Here, we focus on the properties of Eu@C_{72}−4, which has the lowest BE. For Eu@C_{72}−4, the Eu atom is situated away from the center of C_{72} by about 1.40 Å. The C–C bond lengths range from 1.39 Å to 1.49 Å, which differ slightly from those of C_{72}, and the shortest Eu–C bond length is 2.57 Å. In Eu@C_{60} and Eu@C_{82}, Eu ions are positioned slightly away from the center, 1.20 Å [32] for the former and 1.40 Å [33] for the latter. The Eu–C bond lengths in Eu@C_{72} are 0.22 Å shorter than that in $(C_5Me_5)_2Eu$ [34].

The total spin multiplicity of the ground state is S=8. The spin densities on Eu and C_{72} are 6.964 and 0.036, respectively. The spin multiplicities of S=2, 4 and 6,are 386.44, 187.80 and 41.85 kJ mol^{-1} higher respectively, than that of S=8. Figure 2 shows the spatial distribution of spin density for Eu@C_{72}−4. It can be seen from Fig. 2 that the spin densities are distributed over the Eu atom.

Mulliken population analysis shows that the resulting electronic configuration of Eu is $6s^{0.14}$ $4f^{6.972}$ $5d^{0.771}$ and the Mulliken charge on Eu is +0.973e. The occupation of 0.771e on the Eu 5d orbitals is ascribed to a contribution of back-donation of the occupied orbitals of the fullerene cage [35–37]. After this correction, the charge transfer from Eu to C_{72} is about 1.744e, which is close to the experimental result. Therefore, seven electrons spin on the Eu ion and two valance electrons transfer onto the C_{72} cage. The electronic structure of Eu@C_{72} can be described as $Eu^{2+}C_{72}^{2-}$.

In addition to the charge transfer, orbital hybridization between the guest transition-metal/lanthanide atoms and fullerene is another common characteristic of monometallofullerenes [38–41], and we find this to be so in Eu@C_{72}. Figure 3 displays the electron density in a plane containing the Eu atom. Minor electron accumulation leads to weak covalent bond formation between Eu and proximal C atoms. Therefore, the interaction between Eu and C_{72} is primarily ionic with a weak covalent character.

Electrostatic interactions play an important role in determining the position of the positively charged Eu ion. To provide insight into these interactions, the electrostatic potential map inside the C_{2v} C_{72}^{2-} anion was calculated. Figure 4 shows the electrostatic potential map for C_{72}^{2-} in the plane passing through σ_v. It can be seen that the

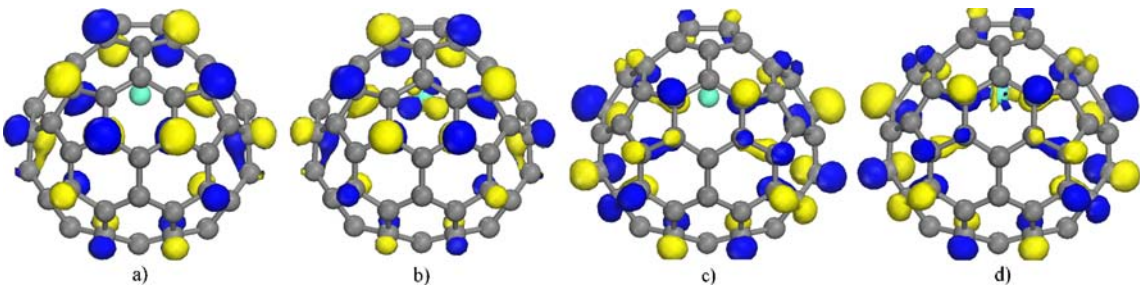

Fig. 5 Isosurfaces (the isovalue is 0.03 a.u.) of: **a** HOMO-1, **b** HOMO, **c** LUMO, **d** LUMO +1 in Eu@C_{72}. *Yellow* and *blue* are used to indicate the positive and negative sign of the wavefunction, respectively (for interpretation of the references to the color in this figure legend, the reader is referred to the web version of this article)

electrostatic potential become more negative upon going from the area near the C–C double bond to the area near the pentagonal ring. This confirms our previous result that Eu@C_{72}−4, in which Eu ion occupies a more negative site, is the most stable structure.

The orbital levels of C_{72} and Eu@C_{72}−4 are shown in Fig. 5. We label the highest carbon-derived occupied state (C-HOMO) and the lowest carbon-derived unoccupied state (C-LUMO) as those occupied (or empty) states nearest to the Fermi level that show barely any weight of the Eu atom [42]. The HOMO-1 and LUMO of Eu@C_{72} should be the C-HOMO and C-LUMO, respectively. The energy difference between the C-HOMO and C-LUMO states is 0.56 eV for Eu@C_{72}, 0.1 eV smaller than that for C_{2v} C_{72}.

To better understand the electronic structure of this endohedral fullerene, the total density of state (TDOS) of Eu@C_{72}−4 is plotted in Fig. 6, together with the TDOS for C_{72} and the partial density of state (PDOS) of Eu in Eu@C_{72}−4. The DOS was obtained by a Lorentzian extension of the discrete energy levels, with weights being the orbital populations in the levels, and a summation over them. The broadening width parameter chosen was 0.20 eV and the Fermi level (E_f) was taken as zero. We explored the hybridized orbitals by analyzing TDOS of Eu@C_{72}−4 and PDOS of Eu in Eu@C_{72}−4. The figure shows that there is no peak of PDOS for Eu in Eu@C_{72}−4 near the E_f, while there are some small peaks appearing in the energy range from −10 to −1 eV, indicating some weak hybridization between the atomic orbitals of Eu and those of the carbons of cage C_{72}.

Finally, to gain insight into the reactivity properties of Eu@C_{72}−4 compared with pristine C_{2v} C_{72}, the vertical ionization potentials (VIPs) and the vertical electron affinities (VEAs) of C_{2v} C_{72} and Eu@C_{72}−4 were calculated. The VIP is the energy difference between positively charged and neutral clusters. The VEA is evaluated by adding one electron to the neutral cluster in its equilibrium geometry and taking the difference between their total energies. The calculated VIP and VEA are 6.56 and 2.88 eV for C_{2v} C_{72}, while the calculated values of VIP and VEA for Eu@C_{72} are 6.62 and 3.28 eV, respectively. Both the VIP and VEA are slightly higher than that of pristine C_{72}, indicating that Eu@C_{72} has a slightly stronger ability to capture electrons and has more difficultly in losing electrons compared with pristine C_{72}. We hope further experiments will confirm our calculations.

Conclusions

All-electron relativistic DFT calculations were performed on nine possible optimized geometries of Eu@C_{72}. Among the possible optimized geometries of Eu@C_{72}, the most favorable endohedral site of Eu is an off-center site along the C_2 axis on the σ_v plane pointing to the (5, 5) bond in the C_{2v} cage. Calculations for electronic structures show that the spin densities are distributed over the Eu ion. Two valance electrons of Eu transfer onto the C_{72} cage, which is in quite good agreement with experimental results. In addition, the Eu ion has little distribution to DOS around E_f.

Acknowledgments We thank the Key Laboratory of Coal Science & Technology (Taiyuan University of Technology), Ministry of Education, for the software. This research was financially supported by State Basic Research Development Program of China (973 program) (Grant No.2004CB217808), National Natural Science Foundation of China (Grant No.90306014, 20671068), Natural Science Foundation of Shanxi Province (Grant No.20050018 and 2006011053)

References

1. Krätschmer W, Lamb LD, Fostiropoulos K, Huffman DR (1990) Nature 347:354–358
2. Hennrich FH, Michel RH, Fischer A, Richard-Schneider S, Gilb S, Kappes MM, Fuchs D, Bürk M, Kobayashi K, Nagase S (1996) Angew Chem Int Ed 35:1732–1734
3. Kroto HW (1987) Nature 329:529–531
4. Ettl R, Chao I, Diederich F, Whetten RL (1991) Nature 353:149–153
5. Diederich F, Whetten RL, Thilgen C, Errl R, Chao I, Alvarez MM (1991) Science 254:1768–1770
6. Kikuchi K, Nakahara N, Wakabayashi T, Suzuki S, Shiromaru H, Miyake Y, Saito K, Ikemoto I, Kainosho M, Achiba Y (1992) Nature 357:142–145
7. Manolopoulos DE, Fowler PW (1992) J Chem Phys 96:7603–7614
8. Kobayashi K, Nagase S (1998) Chem Phys Lett 282:325–329
9. Akasaka T, Wakahara T, Nagase S, Kobayashi K, Waelchli M, Yamamoto K, Kondo M, Shirakura S, Okubo S, Maeda Y, Kato T, Kako M, Nakadaira Y, Nagahata R, Gao X, Caemelbecke EV, Kadish KM (2000) J Am Chem Soc 122:9316–9317
10. Wang CR, Kai T, Tomiyama T, Yoshida T, Kobayashi Y, Nishibori E, Takata M, Sakata M, Shinohara H (2000) Nature 408:426–427
11. Stevenson S, Fowler PW, Heine T, Duchamp JC, Rice G, Glass T, Harich K, Hajdu E, Bible R, Dorn HC (2000) Nature 408:427–428
12. Olmstead MM, Lee HM, Duchamp JC, Stevenson S, Marciu D, Dorn HC, Balch AL (2003) Angew Chem Int Ed 42:900–903
13. Beavers CM, Zuo T, Duchamp JC, Harich K, Dorn HC, Olmstead MM, Balch AL (2006) J Am Chem Soc 128:11352–11353
14. Slanina Z, Ishimura K, Kobayashi K, Nagase S (2004) Chem Phys Lett 384:114–118
15. Slanina Z, Kobayashi K, Nagase S (2003) Chem Phys Lett 372:810–814
16. Slanina Z, Xiang Z, Grabuleda X, Ozawa M, Uhlík F, Ivanov P, Kobayashi K, Nagase S (2001) J Mol Graph Model 19:252–255
17. Wakahara T, Nikawa H, Kikuchi T, Nakahodo T, Rahman GMA, Tsuchiya T, Maeda Y, Akasaka T, Yoza K, Horn E, Yamamoto K, Mizorogi N, Slanina Z, Nagase S (2006) J Am Chem Soc 128:14228–14229
18. Liu XG, Chi M, Han PD, Zhang ZX, Fang XH, Jia W, Xu BX (2007) J Mol Struc (THEOCHEM) 818:71–75
19. Park JK, Ahn JI, Lim MA, Kim CH, Park HD, Choi SY (2003) J Electrochem Soc 150:187–191
20. Schweizer S, Hobbs LW, Secu M, Spaeth JM, Edgar A, Williams GVM (2003) Appl Phys Lett 83:449–451

21. Kuran P, Krause M, Bartl A, Dunsch, L (1998) Chem Phys Lett 292:580–586
22. Sun BY, Inoue T, Shimada T, Okazaki T, Sugai T, Suenaga K, Shinohara H (2004) J Phys Chem B 108:9011–9015
23. Hideto M, Norio O, Takeshi K, Hiroyuki N, Isao I, Koichi K, Ko F, Kazunobu S, Daisuke S, Takeji T, Tatsuhisa K (2004) J Phys Chem B 108:13972–13976
24. Bucher K, Epple L, Mende J, Mehring M, Jansen M (2006) Phys Status Solidi B 243:3025–3027
25. Bucher K, Mende J, Mehring M, Jansen M (2007) Fuller Nanotub Car N 15:29–42
26. Delley B (1990) J Chem Phys 92:508–517
27. Delley B (2000) J Chem Phys 113:7756–7763
28. Delley B (2002) Phys Rev B 66(1–9):155125
29. Perdew JP, Wang Y (1992) Phys Rev B 45:13244–13249
30. Douglas M, Kroll NM (1974) Ann Phys 82:89–155
31. Kobayashi TK, Nagase S, Yoshida M, Osawa E (1997) J Am Chem Soc 119:12693–12695
32. Suzuki S, Kushida M, Amamiya S, Okada S, Nakao K (2000) Chem Phys Lett 327:291–298
33. Mizorogi N, Nagase S (2006) Chem Phys Lett 431:110–112
34. Evance WJ, Hughes LA, Hanusa TP (1986) Organometallics 5:1285–1291
35. Lu J, Sabirianov RF, Mei WN, Gao Y, Duan CG, Zeng XC (2006) J Phys Chem B 110:23637–23640
36. Senapati L, Schrier J, Whaley KB (2004) Nano Lett 4:2073–2078
37. De Nadaï C, Mirone A, Dhesi SS, Bencok P, Brookes NB, Marenne I, Rudolf P, Tagmatarchis N, Shinohara H, Dennis TJS (2004) Phys Rev B 69(1–7):184421
38. Lu J, Zhang X, Zhao X, Nagase S, Kobayashi K (2000) Chem Phys Lett 332:219–224
39. Lu J, Zhang X, Zhao X (2000) Chem Phys Lett 332:51–57
40. Wang K, Zhao J, Yang S, Chen L, Li Q, Wang B, Yang S, Yang J, Hou JG, Zhu Q (2003) Phys Rev Lett 91(1–4):185504
41. Kessler B, Bringer A, Cramn S, Schlebusch C, Eberhardt W, Suzuki S, Achiba Y, Esch F, Barnaba M, Cocco D (1997) Phys Rev Lett 79:2289–2292
42. Lu GL, Deng KM, Wu HP, Yang JL, Wang X (2006) J Chem Phys 124:054305-1-5